

# Preselection algorithm based on predictive control for direct matrix converter

ISSN 1751-8660

Received on 29th July 2016

Revised on 18th October 2016

Accepted on 31st October 2016

doi: 10.1049/iet-epa.2016.0473

www.ietdl.org

Hanbing Dan<sup>1</sup>, Qi Zhu<sup>1</sup> ✉, Tao Peng<sup>1</sup>, Sun Yao<sup>1</sup>, Patrick Wheeler<sup>2</sup>

<sup>1</sup>School of Information Science and Engineering, Central South University, Changsha, People's Republic of China

<sup>2</sup>Department of Electrical and Electronic Engineering, University of Nottingham, Nottingham, UK

✉ E-mail: csu\_zhuqi@163.com

**Abstract:** This study presents an enhanced predictive control strategy to reduce the calculation effort for direct matrix converters. The main idea is to preselect the switching states to decrease the calculation effort during each sample period. The proposed preselection algorithm enables a predefined cost function to consider only the preselected switching states to perform the expected control. On the basis of the preselection of switching states at each sample period, the proposed method can effectively reduce the calculation effort as well as show a good performance. The proposed predictive control scheme uses only preselected switching states to generate the desired source/load current waveforms and control the input power factor. The feasibility of the proposed method is experimentally verified and results are presented in the study.

## 1 Introduction

Power converters are widely used for control in industrial applications including motor drives, energy conversion and power generation. The control of power converters has attracted much attention and several control schemes have been considered. Hysteresis and linear controls coupled with pulse-width modulation, which includes carrier-based modulation and space vector modulation (SVM), are the most mature techniques [1, 2]. Furthermore, some new and complex control schemes have been proposed and implemented due to the development of more advanced microprocessors. These new techniques include fuzzy logic, sliding mode control and predictive control.

The advantages of predictive control present great potential in the control of power converters [3]:

- (i) The concept is comprehensible and the control is easily implemented.
- (ii) The constraints and non-linearities of different systems can be easily satisfied.
- (iii) Multiobjective problems can be simultaneously considered.

The current types of predictive control can be classified into four groups: deadbeat control, hysteresis-based predictive control, trajectory-based predictive control and model predictive control (MPC). MPC includes MPC with a continuous control set and MPC with a finite control set.

Compared with MPC with continuous control sets, MPC with finite control sets directly generates the switching signals of variable frequency without a modulator. Constraints of power converter can be included in predictive control and the methods generally have low implementation complexity. Considering the discrete nature of power converters and the finite set of possible switching states, the optimisation problems of MPC is reduced to the evaluation of all possible switching states and the minimising of the given cost function. When the calculation horizon decreases the calculation of MPC with a finite control set is easier to implement. Hence, the predictive control method based on finite control set has been proposed as a simple and effective control method for power converters [4, 5]. The MPC with a finite control set has been applied for some application including current

control [6–8], torque and flux control [9], power control [10], control of flying capacitor converter [10] and open-switch fault tolerant [11].

The standard matrix converter (MC) [12] with nine bidirectional switches was first proposed by Gyugyi, L in 1970 [13]. The MC has no DC-link energy storage elements, which makes it more compact and potentially more reliable when compared with the back-to-back converter [14]. Due to these advantages it is expected that the MC can be applied in many ac–ac conversion applications, such as integrated motor drives, flexible ac transmission system, and wind energy conversion system [15–17]. Many conventional modulation methods [18], such as carrier-based modulation method, SVM method and modulation strategy based on mathematical constructions have been proposed for the MC. MPC has recently been introduced to simplify the complexity of MC control [19, 20]. It has several advantages such as having a very intuitive approach, no need for linear controllers and modulators, and easy inclusion of non-linearities [21]. This work establishes the models of the converter and load to predict the future values of load current and reactive power. These models are used to decide which switching state is the most suitable to apply for minimising the cost function. Generally, according to the above control schemes, it is possible to summarise the principle of predictive control for MC as follows: (i) All possible switching states are substituted into the discrete models to calculate the future values of source current and load current in the next sampling time, and each predicted value corresponds to a value of cost function. (ii) The switching state producing the minimum value of cost function is selected to apply in the next modulation period. (iii) The performance of MC can be regulated by changing the weighting factors of different terms in the cost function.

In most predictive control algorithms, all possible control actions are evaluated by the cost function and then the optimum control can be taken by using the minimisation of the cost function. Consequently, a certain predictive horizon will be formed by the system's reaction to these control actions. A higher prediction horizon theoretically leads to a better control performance, but the calculation effort rises exponentially. Among most of the predictive control methods for the MC, the easiest way to realise the minimisation of cost function is an evaluation of all the possible switching states [22]. The disadvantage of this method is obvious that the calculation effort rises with the prediction horizon. Hence, an optimal algorithm is needed which will reduce the calculation effort and make possible higher predictive horizons.

In [23] a predictive control algorithm with three or four prediction steps is presented for two-level voltage source inverter (VSI). This algorithm uses a heuristic method to reduce the calculation effort and makes higher predictive horizons feasible in real time. Only the three switching states closest to the continuous-valued optimum solution are evaluated for the first two prediction steps, and only the two closest ones for the third and fourth prediction step. The combinations of switching states decrease from  $7^3 = 343$  to 18 for three prediction steps and from  $7^4 = 2401$  to 36 for four prediction steps. Then the optimisation becomes a search for the right region and the closest switching states. The region selection is completed by a binary search tree, which is effective and time-saving for a higher number of regions. This proposed method significantly reduces the calculation effort for the MPC, and has been applied to reduce the calculation effort for the induction motor (IM) fed by a two-level three-phase VSI in [24].

For a cascaded H-bridge inverter a large number of available voltage vectors make it difficult to implement the MPC algorithm in a standard control platform. In [25] a method is proposed to reduce the set of voltage vectors without degrading the system's performance by two steps. First, the voltage vectors generating the minimum common-mode voltage will be selected. Then, a subset of possible voltage vectors will be selected to drive the inverter by considering information about the previously applied voltage vector. In [26] a distributed MPC strategy was proposed, which is suitable for back-to-back converters and multi-level converters. The controller computational burden is approximately one fourth of classical requirement for FCS-MPC. In [27] a simplified FCS-MPC method solves the 'required voltage' first, which makes the current in the next sampling period equal to its reference. The switching state, which is the closest to the required voltage, is applied to the power converter. The closest switching state is selected by a specialised sector distribution method. Compared with the conventional FCS-MPC using the cost function to select the optimal switching state, the computational complexity of simplified FCS-MPC is greatly reduced and the performance of the simplified FCS-MPC is the same as that of the conventional FCS-MPC.

However, the method developed in [27] cannot be applied to MC directly. For the two-level converter in [27], only the required output voltage is needed to be satisfied. For the MC in this paper, the steady reference is different from that of two-level converter. The required output voltage and input current are both needed to be satisfied for MC. The optimal switching state cannot be selected easily by the specialised sector distribution method in [27]. Thus, this paper proposes an enhanced predictive control strategy, which preselects the switching states at the next sample period according to the

sectors of input current vector and output voltage vector. In conventional predictive control scheme for direct matrix converter (DMC), 27 switching states are considered for the prediction. The proposed preselection algorithm first excludes the impossible switching states and uses 11 preselected switching states to generate the expected source/load current. It can generate good source/load current waveforms and take full control of input power factor. The feasibility of the proposed method is validated using experiment results.

## 2 Direct matrix converter

The DMC consists of 3\*3 matrix bidirectional power semiconductors as shown in Fig. 1. An input filter is used to avoid overvoltage and reduce input current distortion. The following equations explain the modulation principle of the DMC remembering that an open circuit is prohibited across the load connections and a short circuit is prohibited between the input lines.

$$\mathbf{u}_o = \begin{bmatrix} S_{Aa} & S_{Ab} & S_{Ac} \\ S_{Ba} & S_{Bb} & S_{Bc} \\ S_{Ca} & S_{Cb} & S_{Cc} \end{bmatrix} \mathbf{u}_e \quad (1)$$

$$\mathbf{i}_e = \begin{bmatrix} S_{Aa} & S_{Ab} & S_{Ac} \\ S_{Ba} & S_{Bb} & S_{Bc} \\ S_{Ca} & S_{Cb} & S_{Cc} \end{bmatrix}^T \mathbf{i}_o \quad (2)$$

$$\begin{cases} S_{Aa} + S_{Ab} + S_{Ac} = 1 \\ S_{Ba} + S_{Bb} + S_{Bc} = 1 \\ S_{Ca} + S_{Cb} + S_{Cc} = 1 \end{cases} \quad (3)$$

where  $\mathbf{u}_e$ ,  $\mathbf{i}_e$ ,  $\mathbf{u}_o$  and  $\mathbf{i}_o$  present the input voltage, the input current, the output voltage and the load current of the DMC, respectively.  $S_{XY}$  ( $X \in \{A, B, C\}$ ,  $Y \in \{a, b, c\}$ ) equals to '1' when  $S_{XY}$  is turned on and equals to '0' when  $S_{XY}$  is turned off, respectively.

## 3 Principle of predictive control

In the following section all the three phase quantities are assumed to be symmetrical and these can therefore be transformed from the static three-phase coordinates to the static two-phase coordinates. For example, certain three phase quantities  $X_a$ ,  $X_b$  and  $X_c$  are

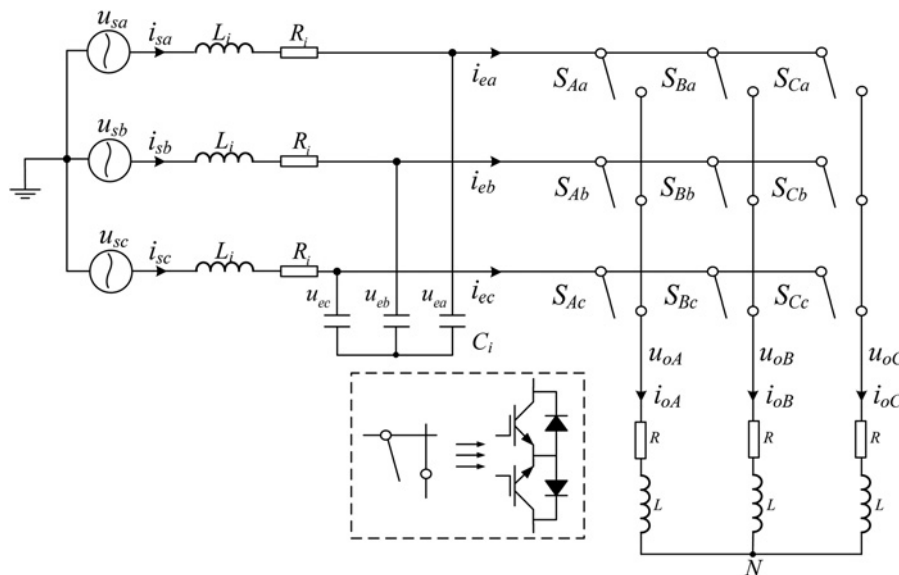


Fig. 1 Topology of the direct MC

re-expressed by the complex space vector

$$X = X_\alpha + j \cdot X_\beta \quad (4)$$

which is defined as

$$\begin{cases} X_\alpha = \frac{1}{3}(2X_a - X_b - X_c) \\ X_\beta = \frac{1}{\sqrt{3}}(X_b - X_c) \end{cases} \quad (5)$$

Predictive control is utilised to select the optimal switching state that makes the controlled variables follow the respective reference during one sample period. For DMC, two main conditions must be satisfied to properly operate: unity power factor and satisfactory steady state performance. The predictive values of the source and load currents are calculated for each possible switching state by measuring the source voltage, the source current, the capacitor voltages and the load current to meet the mentioned objectives. First, the objective of unity power factor can be reduced to keep the source voltage and current in the same phase, as follow

$$g_1 = (i_{s\alpha}^* - i_{s\alpha}^p)^2 + (i_{s\beta}^* - i_{s\beta}^p)^2 \quad (6)$$

where  $i_{s\alpha}^p$  and  $i_{s\beta}^p$  denote the predictive source current in the next sample period and  $i_{s\alpha}^*$  and  $i_{s\beta}^*$  denote the respective references. The phase of source current reference is equal to the phase of source voltage, and the amplitude of source current reference is determined as follow [11]

$$I_{sm}^* = \frac{\eta U_{sm} \pm \sqrt{(\eta U_{sm})^2 - 4\eta R_i R I_{om}^*{}^2}}{2\eta R_i} \quad (7)$$

where  $I_{om}^*$  and  $U_{sm}$  are the amplitude of the reference load current and the source voltage, respectively.  $\eta$  means the efficiency of DMC.

Second, the objective of satisfactory steady state performance can be reduced to minimise the error between the load current prediction and reference

$$g_2 = (i_{o\alpha}^* - i_{o\alpha}^p)^2 + (i_{o\beta}^* - i_{o\beta}^p)^2 \quad (8)$$

where  $i_{o\alpha}^p$  and  $i_{o\beta}^p$  denote the predictive load current in the next sample period and  $i_{o\alpha}^*$  and  $i_{o\beta}^*$  denote the respective references. Equations (6) and (8) are merged into a cost function

$$g = \lambda_1 \cdot g_1 + \lambda_2 \cdot g_2 \quad (9)$$

where  $\lambda_1$ ,  $\lambda_2$  are the weighing factors deciding the priority of corresponding control variable, which are flexibly changed due to different control requirements. At each sample period, all possible switching states are substituted into (9) to calculate  $g$ . The switching state generating the minimum value of  $g$  is selected to be implemented for the next sample period.

#### 4 Calculation of predictive values

The predictions of source and load currents, which are necessary for evaluating the cost function  $g$ , can be derived from the mathematical models of input filter and load.

The mathematical model of the input filter is related to the source voltage, input voltage, source current and input current, and the

following state-space system describe the input filter model

$$\begin{bmatrix} \frac{du_e}{dt} \\ \frac{di_s}{dt} \end{bmatrix} = A \begin{bmatrix} u_e \\ i_s \end{bmatrix} + B \begin{bmatrix} u_s \\ i_e \end{bmatrix} \quad (10)$$

$$A = \begin{bmatrix} 0 & \frac{1}{C_i} \\ -\frac{1}{L_i} & -\frac{R_i}{L_i} \end{bmatrix}, B = \begin{bmatrix} 0 & -\frac{1}{C_i} \\ \frac{1}{L_i} & 0 \end{bmatrix} \quad (11)$$

where the  $u_s$ ,  $u_e$ ,  $i_s$ ,  $i_e$  represent the source voltage, input voltage, source current and input current, respectively.  $R_i$ ,  $L_i$ ,  $C_i$  represent the resistances, inductances and capacitance of the mains and filter, respectively. Further, assuming the sample period is  $T_s$ , the state-space system is discretised by forward Euler approximation and the predictions of capacitor voltage and source current are obtained as follow

$$\begin{bmatrix} u_e^{k+1} \\ i_s^{k+1} \end{bmatrix} = e^{AT_s} \begin{bmatrix} u_e^k \\ i_s^k \end{bmatrix} + A^{-1}(e^{AT_s} - I)B \begin{bmatrix} u_s^k \\ i_e^k \end{bmatrix} \quad (12)$$

The load model is related to the output voltage and load current, and the following state-space system describes the load model

$$L \frac{di_o}{dt} = u_o - Ri_o \quad (13)$$

which is discretised in the same way as follow

$$i_o^{k+1} = u_o^k \frac{T_s}{L} + \left(1 - \frac{T_s R}{L}\right) i_o^k \quad (14)$$

Above all, all the prediction equations are rewritten as follows

$$\begin{cases} u_e^{k+1} = L_{11}u_e^k + L_{12}i_s^k + M_{11}u_s^k + M_{12}i_e^k \\ i_s^{k+1} = L_{21}u_e^k + L_{22}i_s^k + M_{21}u_s^k + M_{22}i_e^k \\ i_o^{k+1} = N_1u_o^k + N_2i_o^k \end{cases} \quad (15)$$

where

$$\begin{bmatrix} L_{11} & L_{12} \\ L_{21} & L_{22} \end{bmatrix} = e^{AT_s}, \begin{bmatrix} M_{11} & M_{12} \\ M_{21} & M_{22} \end{bmatrix} = A^{-1}(e^{AT_s} - I)B, \begin{cases} N_1 = \frac{T_s}{L} \\ N_2 = 1 - \frac{T_s R}{L} \end{cases}$$

#### 5 Proposed predictive control with preselection algorithm

For the conventional predictive method, all these 27 switching states will be substituted into the cost function for optimum selection. A complete enumeration of all possible switching states leads to more online calculation time. In order to reduce the necessary online computation time, an optimised predictive control method with the vector preselection is proposed to narrow down the range of possible switching states, instead of numerating all switching states. The proposed predictive control method is based on the instantaneous space vector representation of input currents and output voltages. Different switching states will be substituted into the cost function for optimum selection when the input current vector and the output voltage vector lie in different sectors, respectively.

According to the output voltage vector and input current vector that each switching state generates, the 27 switching states are

**Table 1** Possible switching states and their space vectors

Group no.	Switching states	A B C	$U_{om}$	$\alpha_o$	$I_{im}$	$\beta_i$
I	+1	a b b	$2u_{eab}/3$	0	$2i_a/\sqrt{3}$	$-\pi/6$
I	-1	b a a	$-2u_{eab}/3$	0	$-2i_a/\sqrt{3}$	$-\pi/6$
I	+2	b c c	$2u_{ebc}/3$	0	$2i_b/\sqrt{3}$	$\pi/2$
I	-2	c b b	$-2u_{ebc}/3$	0	$-2i_b/\sqrt{3}$	$\pi/2$
I	+3	c a a	$2u_{eca}/3$	0	$2i_c/\sqrt{3}$	$7\pi/6$
I	-3	a c c	$-2u_{eca}/3$	0	$-2i_c/\sqrt{3}$	$7\pi/6$
I	+4	b a b	$2u_{eab}/3$	$2\pi/3$	$2i_b/\sqrt{3}$	$-\pi/6$
I	-4	a b a	$-2u_{eab}/3$	$2\pi/3$	$-2i_b/\sqrt{3}$	$-\pi/6$
I	+5	c b c	$2u_{ebc}/3$	$2\pi/3$	$2i_b/\sqrt{3}$	$\pi/2$
I	-5	b c b	$-2u_{ebc}/3$	$2\pi/3$	$-2i_b/\sqrt{3}$	$\pi/2$
I	+6	a c a	$2u_{eca}/3$	$2\pi/3$	$2i_c/\sqrt{3}$	$7\pi/6$
I	-6	c a c	$-2u_{eca}/3$	$2\pi/3$	$-2i_c/\sqrt{3}$	$7\pi/6$
I	+7	b b a	$2u_{eab}/3$	$4\pi/3$	$2i_c/\sqrt{3}$	$-\pi/6$
I	-7	a a b	$-2u_{eab}/3$	$4\pi/3$	$-2i_c/\sqrt{3}$	$-\pi/6$
I	+8	c c b	$2u_{ebc}/3$	$4\pi/3$	$2i_d/\sqrt{3}$	$\pi/2$
I	-8	b b c	$-2u_{ebc}/3$	$4\pi/3$	$-2i_d/\sqrt{3}$	$\pi/2$
I	+9	a a c	$2u_{eca}/3$	$4\pi/3$	$2i_d/\sqrt{3}$	$7\pi/6$
I	-9	c c a	$-2u_{eca}/3$	$4\pi/3$	$-2i_d/\sqrt{3}$	$7\pi/6$
II	0	a a a	0	-	0	-
II	0	b b b	0	-	0	-
II	0	c c c	0	-	0	-
III	-	a b c	$U_{em}$	$\alpha_i$	$I_{om}$	$\beta_o$
III	-	a c b	$-U_{em}$	$-\alpha_i$	$I_{om}$	$-\beta_o$
III	-	b a c	$-U_{em}$	$-\alpha_i + 4\pi/3$	$I_{om}$	$-\beta_o + 2\pi/3$
III	-	b c a	$U_{em}$	$\alpha_i + 4\pi/3$	$I_{om}$	$\beta_o + 2\pi/3$
III	-	c a b	$U_{em}$	$\alpha_i + 2\pi/3$	$I_{om}$	$\beta_o + 4\pi/3$
III	-	c b a	$-U_{em}$	$-\alpha_i + 2\pi/3$	$I_{om}$	$-\beta_o + 4\pi/3$

classified into three groups as shown in Table 1, where  $u_{eil}$  ( $i, l \in \{a, b, c\}, i \neq l$ ) represents the line-to-line input voltage,  $I_{om}$ ,  $U_{em}$  are the amplitude of the load current and the input voltage, respectively.

Group I: Two output phases are connected to a common input phase, and the third is connected to a different input phase. This group includes 18 switching states which represent the active vectors and determine the output voltage vector and input current vector.

Group II: All three output phases are connected to the same input phase. This group includes three switching states which determine zero input current and output voltage vectors.

Group III: Each output phase is connected to different input phase, respectively. In this group, the output voltage and input current vectors have variable directions and amplitudes. Thus, the remaining six switching states are difficult to synthesise the reference vectors.

As shown in Fig. 2, the complex plane is divided into six sectors by six active voltage vectors. At any sample period, the reference output voltage  $u_o^*$  can be calculated from the reference load current  $i_s^*$  and the resistance-inductance load. The reference input current  $i_e^*$  can be obtained from the source voltage  $u_s$  and the reference source current  $i_s^*$ . The following equations describe the relationship among the quantities above.

$$u_o^* = (R + j\omega_o L)i_o^* \quad (16)$$

$$\begin{cases} u_s = u_e + (R_i + j\omega_i L_i)i_s^* \\ i_s^* = i_c + i_e^* \\ i_c = j\omega_i C_i u_e \end{cases} \quad (17)$$

where  $R$  and  $L$  are the load resistance and inductance, respectively.  $L_i$  comprises the mains and filter inductances,  $R_i$  represents the mains and filter resistances and  $C_i$  is the filter capacitance. For the preselection of the finite control set, it is necessary to judge the sector of the vector  $u_o^*$  and  $i_e^*$ . Assume the input power factor is unity, the angle of the vector  $u_o^*$  and  $i_e^*$  can be calculated as follows.

$$\alpha_{io} = \alpha_{io} + \arctan \frac{\omega_o L}{R} \quad (18)$$

$$\beta_{ie} = \beta_{is} + \arctan \frac{-\omega_i C_i (u_s - R_i i_s^*)}{(1 - \omega_i^2 C_i^2) i_s^*} \quad (19)$$

where  $\alpha_{io}$  is the angle of the vector  $u_o^*$ ,  $\alpha_{io}$  is the angle of the vector  $i_o^*$ .  $\beta_{ie}$  is the angle of the vector  $i_e^*$  and  $\beta_{is}$  is the angle of the source  $i_s^*$ .

To clearly explain the method of preselecting the finite control set, the reference vectors  $u_o^*$  and  $i_e^*$  are both assumed to be located in sector I as shown in Figs. 2a and b. The reference voltage vector  $u_o^*$  is resolved into two adjacent vectors  $u_o^{*'} and  $u_o^*$ . The vector  $u_o^*$  can be synthesised with the voltage vectors which correspond to the pairs of switching configurations  $\pm 1, \pm 2, \pm 3$ . These voltage vectors have the same direction with  $u_o^{*'}$ . At the same time, the six switching states of  $u_o^*$  are  $\pm 7, \pm 8, \pm 9$ . Similarly, the reference input current vector  $i_e^*$  is obtained from two adjacent vectors  $i_e^{*'}$  and  $i_e^*$  which are generated by switching configurations  $\pm 3, \pm 6, \pm 9$  and  $\pm 1, \pm 4, \pm 7$ . However, only the common switching states between the output voltage and input current vectors will be considered in the finite control set because they are synthesised at the same sample period. As a result, the switching states  $\pm 2$  and  $\pm 8$  are eliminated and the switching configurations  $\pm 1, \pm 3, \pm 7, \pm 9$  will be selected in the finite control set.$

In the same way, it is possible to determine the eight switching states related to any possible combination of output voltage and input current sectors. On the other hand, the three switching states from group II are chosen in each finite control set because the zero input current and output voltage vectors are useful for the proposed predictive control method. The preselected switching states are summarised in Table 2. In Fig. 3, the block diagram of the predictive control strategy applied on DMC is described. At the  $k$ th sample period  $T^k$ , the angles of reference input current vector and the reference output voltage vector are computed from (18) and (19). With the angle of the vector  $i_e^*$  and  $u_o^*$ , it is easy to judge the sectors of  $i_e^*$  and  $u_o^*$ . There are 11 switching states chosen in the preselected finite control set. At the same time, the variables  $u_s^k, i_s^k, u_e^k$  and  $i_o^k$  in  $T^k$  are obtained from the sensor circuits, and the switching states  $S^k$  in  $T^k$  is obtained from the previous sample period. The variables  $i_e^k$  and  $u_o^k$  are calculated according to the MC model. Thus,  $i_o^{k+1}, i_s^{k+1}$  and  $u_e^{k+1}$  at the  $(k+1)$ th sample period  $T^{k+1}$  can be derived according to the load model and the input filter model, respectively.  $u_s^{k+1}$  is considered equal to  $u_s^k$  ignoring the change of the source voltage in a small sample period. In the same way, predictive values of  $i_o^{k+2}$  and  $i_s^{k+2}$  at the  $(k+2)$ th sample period  $T^{k+2}$  can be obtained for each valid switching state. Substituting each predictive value into  $g^{k+2}$ , the switching state making  $g^{k+2}$  minimal will be applied in the  $(k+1)$ th sample period  $T^{k+1}$ .

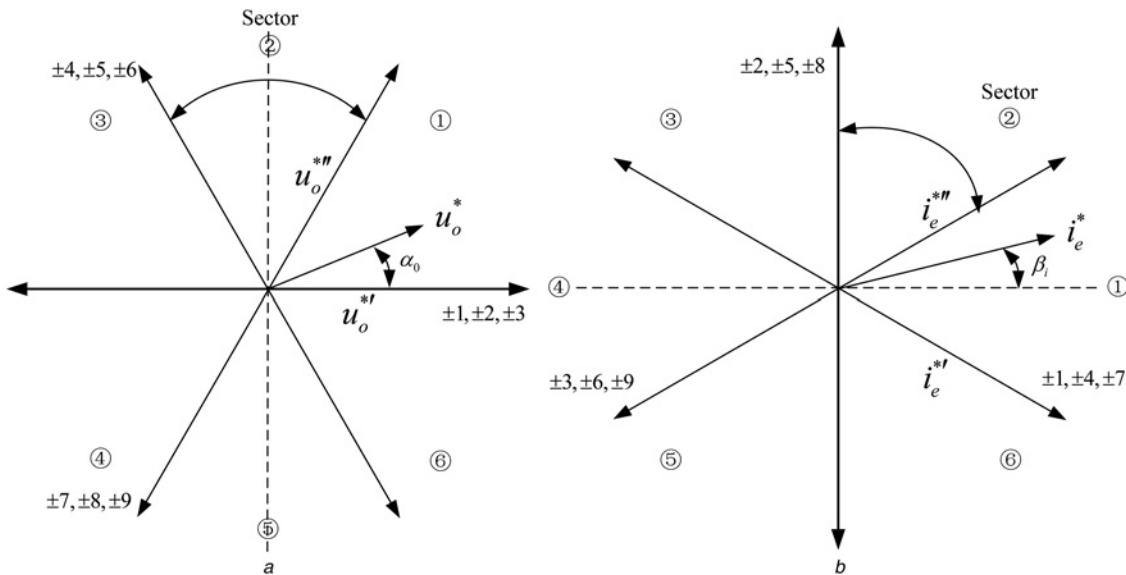


**Fig. 2** Complex plane is divided into six sectors by six active voltage vectors  
*a* Output voltage vectors generated by the active switching states  
*b* Input current vectors generated by the active switching states

**Table 2** Selection of the switching configurations for each combination of output voltage and input current sectors

Preselected switching states	Sector of the output voltage vector		
	1 or 4	2 or 5	3 or 6
Sector of the input current vector	1 or 4	2 or 5	3 or 6
	0, ±1, ±3, ±7, ±9	0, ±4, ±6, ±7, ±9	0, ±1, ±3, ±4, ±6
	0, ±2, ±3, ±8, ±9	0, ±5, ±6, ±8, ±9	0, ±2, ±3, ±5, ±6
	0, ±1, ±2, ±7, ±8	0, ±4, ±5, ±7, ±8	0, ±1, ±2, ±4, ±5

**Table 3** Parameters of the low-voltage experimental prototype

Parameters	Value
source phase voltage ( $V_{RMS}$ )	60 V
source voltage frequency ( $f_n$ )	50 Hz
input mains and filter inductor ( $L_i$ )	0.6 mH
input filter capacitor ( $C_i$ )	66 $\mu$ F
input mains and filter resistor ( $R_i$ )	0.1 $\Omega$
input passive damping resistor ( $R_p$ )	9 $\Omega$
resistor of load ( $R$ )	4.4 $\Omega$
inductor of load ( $L$ )	6 mH

## 6 Experimental results

The operation of the DMC using MPC with the preselection algorithm has been experimental validated using a prototype converter. Using the full schematic model of the system, all the experiments are performed with a symmetrical three phase source. The setup is fed at 50 Hz and the output fundamental frequency was chosen as 40 or 60 Hz in order to ensure the universality of the experiments. Relevant parameters of the experimental converter are presented in Table 3. The power source is not perfect

and hence the AC source voltages contain some undesirable fifth-order and seventh-order harmonics. Thus, the value of  $R_p$  is chosen as 9  $\Omega$ , slightly higher than the ideal value. The bi-directional switches are implemented using IGBT modules, FF200R12KT3\_E. Sensor circuits are equipped to provide the information of the source voltage, the source current, the capacitor voltage and the load current. A floating-point digital signal processor (DSP, TMS320F28335) is used to select the optimal switching state while a field programmable gate array (EP2C8T144C8N) is used for generating a set of impulses to

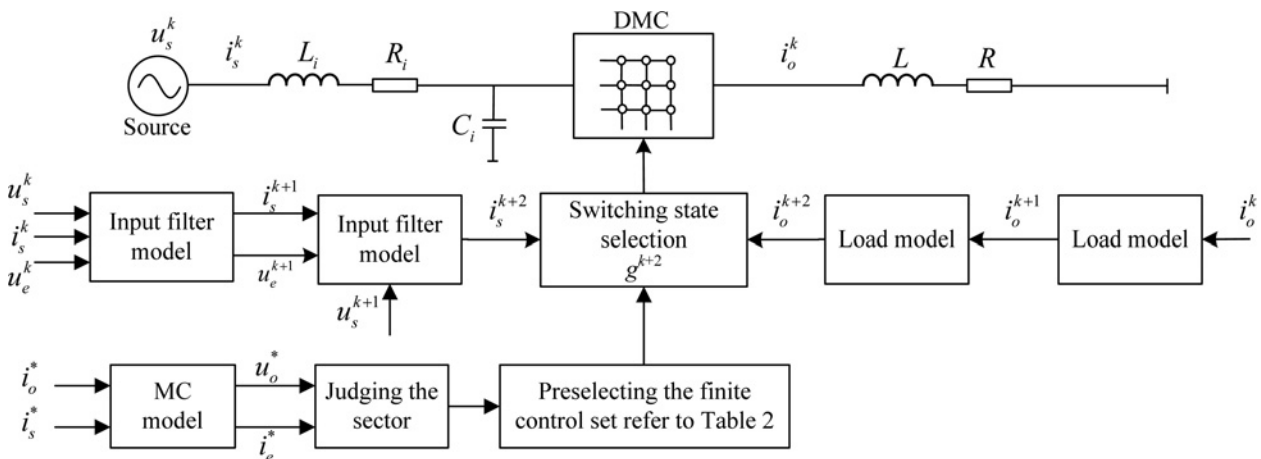


**Fig. 3** Block diagram of the predictive control strategy

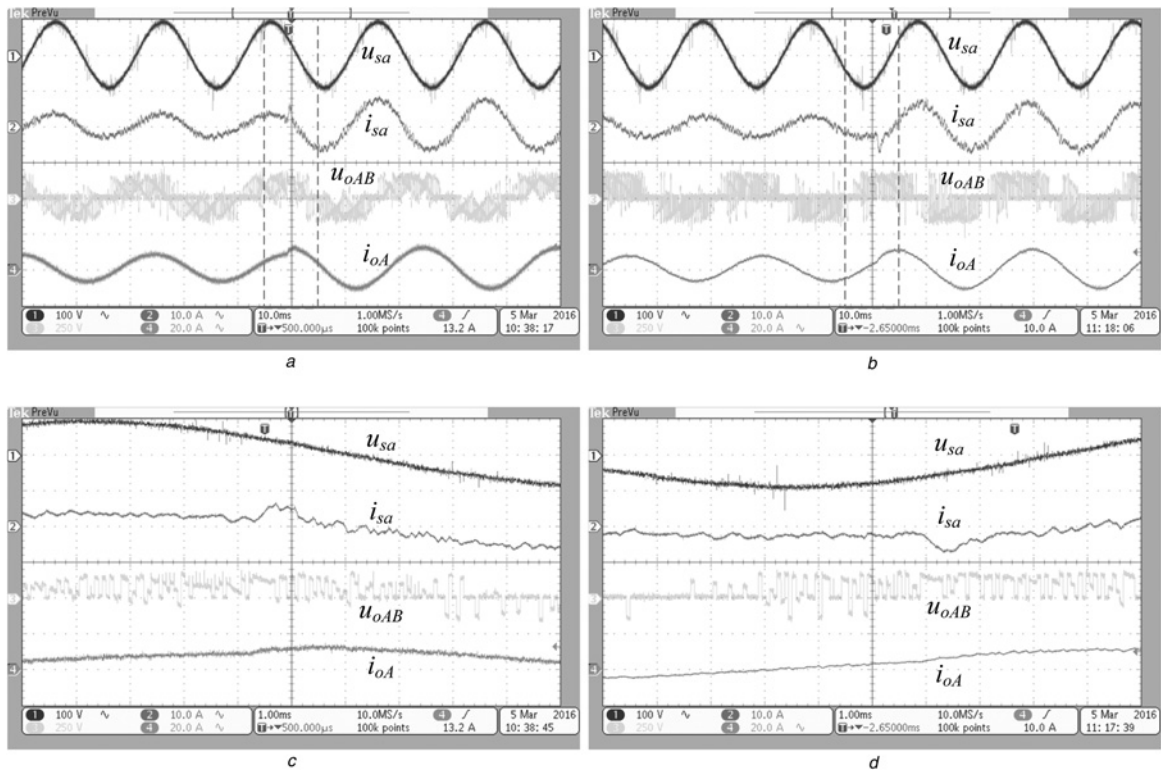


**Fig. 4** Experiment results with  $T_s = 70 \mu\text{s}$  when the reference load current changes from  $I_{om}^* = 8 \text{ A}$ ,  $f_o = 40 \text{ Hz}$  to  $I_{om}^* = 12 \text{ A}$ ,  $f_o = 40 \text{ Hz}$

- a Conventional method
- b Proposed method
- c Enlarged drawing of the dotted box in (a)
- d Enlarged drawing of the dotted box in (b)

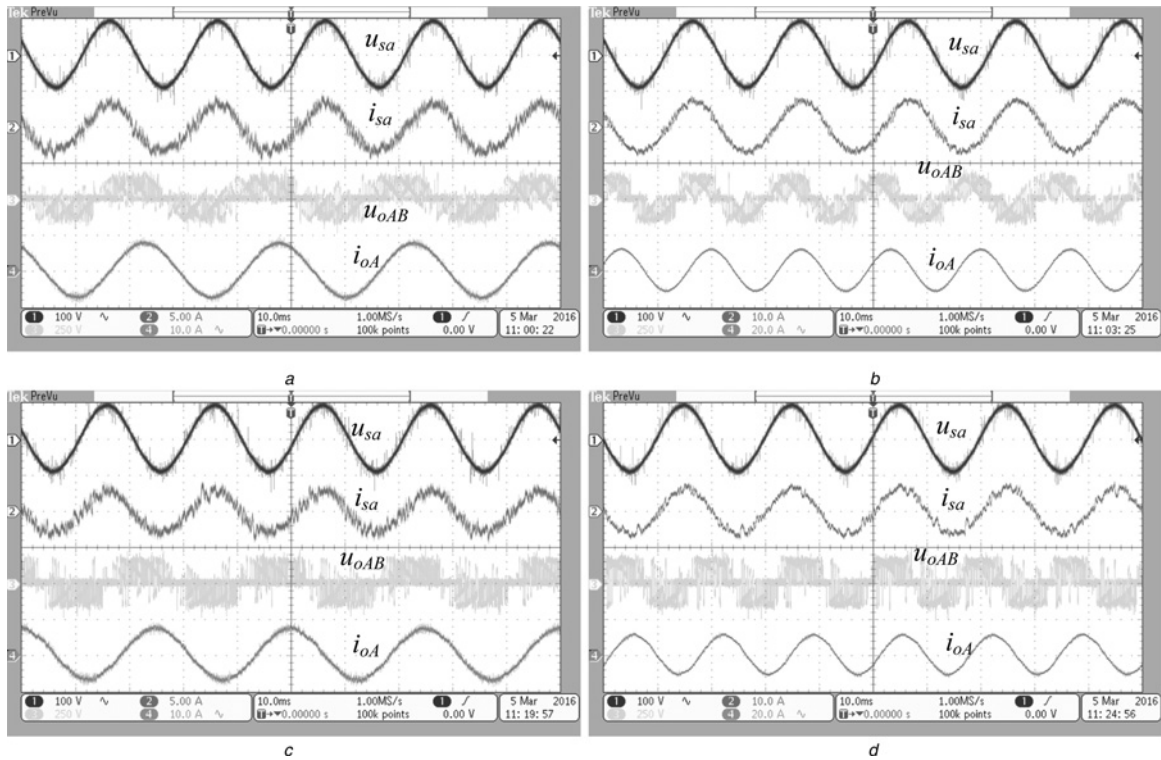


**Fig. 5** Experiment results with  $T_s = 70 \mu\text{s}$

- Conventional method
- a  $I_{om}^* = 8 \text{ A}$ ,  $f_o = 40 \text{ Hz}$
- b  $I_{om}^* = 12 \text{ A}$ ,  $f_o = 60 \text{ Hz}$
- Proposed method
- c  $I_{om}^* = 8 \text{ A}$ ,  $f_o = 40 \text{ Hz}$
- d  $I_{om}^* = 12 \text{ A}$ ,  $f_o = 60 \text{ Hz}$

**Table 4** Comparison between the running time required by the conventional method and the proposed method

Case ( $T_s = 70 \mu\text{s}$ )	Time, $\mu\text{s}$			
	A/D conversion	FCS-MPC algorithm	Other algorithms	Free
conventional method	2.63	55.25	4.42	5.90
proposed method	2.63	26.50	4.60	36.27

**Table 5** THD values of the source current and the load current

Cases			Source current THD, %	Load current THD, %
	Desired load current, Hz	Sample period, $\mu\text{s}$		
8 A, 40	70	conventional	18.04	3.51
		proposed	18.97	4.58
10 A, 50	70	conventional	12.16	3.13
		proposed	13.22	4.13
12 A, 60	70	conventional	8.44	2.17
		proposed	10.04	3.44
14 A, 70	70	conventional	7.47	2.07
		proposed	9.35	3.17

control the switches. The floating-point DSP can also show the computation time of the system.

The experiment results comparing the conventional and proposed method are shown in Fig. 4 when the amplitude of the reference load current changes.  $u_{sa}$ ,  $i_{sa}$ ,  $u_{oAB}$  and  $i_{oA}$  represent the source voltage, the source current, the output line-to-line voltage and the load current, respectively. For the conventional method, 27 switching states are evaluated in the cost function while only 11 switching states are considered for the proposed method. The enlarged drawings of the dotted box in Figs. 4a and c are shown in Figs. 4b and d, respectively. The transient response time of the proposed method in Figs. 4b and d is about 0.4 ms, which is similar to the conventional method in Figs. 4a and c.

The experiment results of the proposed method with different reference load current are shown in Fig. 5. At the same time, the conventional method is also experimented to make a comparison. Furthermore, experiments are performed to show a good result with the unit power factor and the load current following the reference accurately. Because 27 switching states are considered for the conventional method while only 11 switching states are considered for the preselection algorithm. The computation time of the conventional method for DSP (TMS320F28335) is about 64.1  $\mu\text{s}$  while the less computation time 33.73  $\mu\text{s}$  is taken by the preselection algorithm. The detailed comparison between the running time required by the conventional method and the proposed method are shown in Table 4. Experimental results with the same  $I_{om}^*/f_o$  value are performed. The THD values of the source current and the load current with conventional method ( $T_s = 70 \mu\text{s}$ ) and proposed method ( $T_s = 70 \mu\text{s}$ ) are described in Table 5. The THD values of the proposed method with  $T_s = 70 \mu\text{s}$  are a little larger than those of the conventional method with  $T_s = 70 \mu\text{s}$ .

The experimental waveforms of the proposed method show almost the same performance as that of the conventional method. Because of the time the preselection algorithm saves, it is possible to implement the total algorithm on microcontroller, which is cheaper and has lower calculating speed. In other words, these time savings allow the microcontroller to implement some other operations in only one sample period. When the prediction horizon increases, the proposed method will have larger advantage on calculation time compared with the conventional predictive method. Certainly, if high performance is required and the cost of microcontroller is negligible, the conventional method should be considered.

## 7 Conclusion

In this paper a predictive control method with a preselection algorithm for DMC is proposed. On the premise of satisfying the conditions of unity input power factor and accurately following the output current reference value, the proposed control method can reduce the calculation effort for the MPC. The proposed method could also be used with a shorter sample period because of lower computation time. The proposed method preselects the finite control set by judging the sectors of the input current vector and the output voltage vector. Only the switching states in the preselected finite control set are considered while the conventional predictive control method enumerates all the switching states satisfying the restriction of the MC topology. The proposed method allows the regulation of the input power factor by controlling the phase shift between the source current and the source voltage. The experiment results validate the feasibility of the method.

## 8 References

- Kazmierkowski, M.P., Krishnan, R., Blaabjerg, F.: 'Control in power electronics' (New York, 2002)
- Mohan, N., Undeland, T.M., Robbins, W.P.: 'Power electronics' (Wiley Press, Hoboken, New Jersey, 1995, 2nd edn.)
- Cortés, P., Kazmierkowski, M.P., Kennel, R.M., et al.: 'Predictive control in power electronics and drives', *IEEE Trans. Ind. Electron.*, 2008, **55**, (12), pp. 4312–4324
- Kouro, S., Cortes, P., Vargas, R., et al.: 'Model predictive control, a simple and powerful method to control power converters', *IEEE Trans. Ind. Electron.*, 2009, **56**, (6), pp. 1826–1838
- Kouro, S., Perez, M.A., Rodriguez, J., et al.: 'Model predictive control: mpc's role in the evolution of power electronics', *IEEE Trans. Ind. Electron.*, 2014, **9**, (4), pp. 8–21
- Rivera, M., Rojas, C., Rodriguez, J., et al.: 'Methods of source current reference generation for predictive control in a direct matrix converter', *IET Power Electron.*, 2013, **6**, (5), pp. 894–901
- Rivera, M., Rojas, C., Wilson, A., et al.: 'Review of predictive control methods to improve the input current of an indirect matrix converter', *IET Power Electron.*, 2014, **7**, (4), pp. 886–894
- Uddin, M., Mekhilef, S., Rivera, M.: 'Experimental validation of minimum cost function-based model predictive converter control with efficient reference tracking', *IET Power Electron.*, 2015, **8**, (2), pp. 278–287
- Uddin, M., Mekhilef, S., Rivera, M., et al.: 'Imposed weighting factor optimization method for torque ripple reduction of im fed by indirect matrix converter with predictive control algorithm', *J. Electr. Eng. Technol.*, 2015, **10**, (1), pp. 227–242
- Jasinski, M., Kazmierkowski, M., Malinowski, M.: 'Model predictive control for 3-level 4-leg flying capacitor converter operating as shunt active power filter'. Proc. Int. Conf. Industrial Technology, Seville, Spain, March 2015
- Peng, T., Dan, H., Yang, J., et al.: 'Open-switch fault diagnosis and fault tolerant for matrix converter with finite control set-model predictive control', *IEEE Trans. Ind. Electron.*, 2016, **63**, (9), pp. 5953–5863
- Wheeler, P.W., Rodriguez, J., Clare, J.C., et al.: 'Matrix converters: a technology review', *IEEE Trans. Ind. Electron.*, 2002, **49**, (2), pp. 276–288
- Gyugyi, L.: 'Generalized theory of static power frequency changers', PhD thesis, University of Salford, 1970
- Koiwa, K., Itoh, J.I.: 'A maximum power density design method for nine switches matrix converter using sic-mosfet', *IEEE Trans. Power Electron.*, 2016, **31**, (2), pp. 1189–1202
- Abebe, R., Vakili, G., Giovanni, L.C.: 'Integrated motor drives: state of the art and future trends', *IET Electr. Power Appl.*, 2016, **10**, (8), pp. 757–771
- Monteiro, J., Silva, J.F., Pinto, S.F., et al.: 'Matrix converter-based unified power-flow controllers: Advanced direct power control method', *IEEE Trans. Power Deliv.*, 2011, **26**, (1), pp. 420–430
- Suman, M., Debaprasad, K.: 'Improved direct torque and reactive power control of a matrix converter fed grid connected doubly fed induction generator', *IEEE Trans. Ind. Electron.*, 2015, **62**, (12), pp. 7590–7595
- Rodriguez, J., Rivera, M., Kolar, J.W., et al.: 'A review of control and modulation methods for matrix converters', *IEEE Trans. Ind. Electron.*, 2012, **59**, (1), pp. 58–70
- Rivera, M., Wheeler, P.W., Olloqui, A.: 'Predictive control in matrix converters - Part I: Principles, topologies and applications'. Proc. Int. Conf. Industrial Technology, Taipei, Taiwan, March 2016
- Rivera, M., Wheeler, P.W., Olloqui, A.: 'Predictive control in matrix converters - Part II: Control strategies, weaknesses and trends'. Proc. Int. Conf. Industrial Technology, Taipei, Taiwan, March 2016
- Muller, S., Ammann, U., Rees, S.: 'New time-discrete modulation scheme for matrix converters', *IEEE Trans. Ind. Electron.*, 2005, **52**, (6), pp. 1607–1615
- Linder, A., Kanchan, R., Kennel, R., et al.: 'Model-based predictive control of electric drives' (Cuvillier Verlag, 2010)
- Stolze, P., Landsmann, P., Kennel, R., et al.: 'Finite-set model predictive control with heuristic voltage vector preselection for higher prediction horizons'. Proc. Int. Conf. Power Electronics and Applications, Birmingham, United Kingdom, September 2011

- 24 Stolze, P., Tomlinson, M., Kennel, R., *et al.*: 'Heuristic finite-set model predictive current control for induction machines'. Proc. Int. Conf. ECCE Asia Downunder, Melbourne, Australia, June 2013, pp. 1221–1226
- 25 Cortés, P., Wilson, A., Kouro, S., *et al.*: 'Model predictive control of multilevel cascaded h-bridge inverters', *IEEE Trans. Ind. Electron.*, 2010, **57**, (8), pp. 2691–2699
- 26 Tarisciotti, L., Calzo, G.L., Gaeta, A., *et al.*: 'A distributed model predictive control strategy for back-to-back converters', *IEEE Trans. Ind. Electron.*, 2016, **63**, (9), pp. 5869–5878
- 27 Xia, C., Liu, T., Shi, T., *et al.*: 'A simplified finite-control-set model-predictive control for power converters', *IEEE Trans. Ind. Inf.*, 2014, **10**, (2), pp. 991–1002